Service Provisioning in Wavelength-Switched Optical Networks based on P2MP Transceivers

(Invited Paper)

Ruoxing Li, Sijia Li, and Zuqing Zhu*
University of Science and Technology of China, Hefei, China
*Email: zqzhu@ieee.org

***Abstract*—We address the challenge of provisioning dynamic requests in a wavelength-switched optical network (WSON) built with coherent point-to-multipoint transceivers (P2MP-TRXs) in this work. An efficient heuristic for transceiver, routing, and spectrum assignment (TRSA) is proposed, along with a subcarrier (SC) level proactive defragmentation method that can further enhance the provisioning performance through reconfiguring the spectrum allocations of leaf P2MP-TRXs. Extensive simulations confirm the effectiveness of our proposals.**

***Index Terms*—Dynamic provisioning, Point-to-multipoint (P2MP) transceiver, Routing and spectrum assignment.**

I. Introduction

Over past decades, optical networks have undergone tremendous changes for better adaptability and higher cost-efficiency and to meet the ever-growing traffic demands in the Internet [1–4]. One of the representative advances in this evolution is the development of elastic optical networks (EONs) [5–10], which has enabled more spectrally-efficient and cost-effective data transmissions and significantly enhanced the agility of wavelength-switched optical networks (WSONs). However, as the per-channel data-rate of optical networks will soon reach Tbps, communication service providers (CSPs) have to search for new cost-efficient optical networking technologies consistently to reduce cost per bit (CpB) [11].

While state-of-art point-to-point transceivers (P2P-TRXs) continue to reduce the CpB of bandwidth-intensive unicast flows in core networks, the deployment of these P2P-TRXs may become less preferable in other network segments such as metro-aggregation networks. The rationale behind this is two-fold. First, traffic demands in these network segments show distinct hub-and-spoke (H&S) patterns [12, 13], *i.e.*, a hub node often needs to talk with multiple leaf nodes simultaneously. Second, driven by the development of emerging network services [14–16], traffic demands in these segments are becoming more and more dynamic, and thus frequent bandwidth reallocation needs to be triggered to cope with traffic fluctuations [17]. Hence, a CSP needs to deploy a large number of P2P-TRXs in pairs, which results in sub-optimal P2P-TRX usage and hinders further optimization of capital expenditures (CAPEX) and operating expenses (OPEX).

Recent advances on point-to-multipoint transceivers (P2MP-TRXs) have provided a promising alternative to handle dynamic H&S traffic with better cost-efficiency [18]. Enabled by digital subcarrier modulation (DSCM), these P2MP-TRXs can achieve a finer granularity in spectrum allocation by generating a set of low-rate Nyquist subcarriers (SCs) (*e.g.*, at 4 GBaud [18]), while maintaining the complexity and cost similar to their P2P counterparts [13]. Then, significant cost reduction can be achieved in the WSONs for metro-aggregation networks, if we replace P2P-TRXs with P2MP-TRXs in the phase of network planning [19, 20]. Moreover, the working status of SCs from a P2MP-TRX can be adjusted on the fly, making it also beneficial for dynamic service provisioning [21].

Nevertheless, to the best of our knowledge, dynamic service provisioning in P2MP-TRX-based WSONs has not been fully explored yet. Specifically, to satisfy the ever-increasing dynamic traffic in metro-aggregation networks, lightpaths (LPs) between P2MP-TRXs need to be set up and torn down frequently [17]. This will fragment the optical spectra in a WSON to cause spectral discontinuity and misalignment and make the spectra difficult to be reused [22]. Specifically, as multiple low-speed leaf P2MP-TRXs need to use the SCs from the same hub P2MP-TRX, their spectrum usages can only vary in a fixed spectral range, and thus if the SCs are not allocated properly, the induced spectrum fragmentation can decrease the utilizations of both P2MP-TRXs and optical spectra.

In this work, we study the dynamic service provisioning in P2MP-TRX-based WSONs, and propose algorithms to maximize the provision capability of a WSON while maintaining its OPEX at a reasonable level. Specifically, an efficient heuristic is first designed to tackle the transceiver, routing and spectrum assignment (TRSA) in a P2MP-TRX-based WSON, and then an SC-level proactive spectrum defragmentation algorithm is developed to further enhance the spectrum utilization by periodically improving the compactness of occupied spectra and SCs through leaf P2MP-TRX reconfigurations. Extensive simulations verify the effectiveness of our proposals.

II. Network Model

We denote the topology of a WSON as a graph $G(V, E)$, where V and E are the sets of nodes and fiber links, respectively. Each node $v \in V$ is assumed to be equipped with a broadcast-and-select-capable wavelength switch [11], and can serve as either a hub node, a leaf node, or both to satisfy the traffic demands. For the sake of clarity, we treat a hub P2MP-TRX and all of its leaf P2MP-TRXs as a group, where the LPs between them are established in a leader-follower approach. Specifically, a hub P2MP-TRX broadcasts its SCs through the

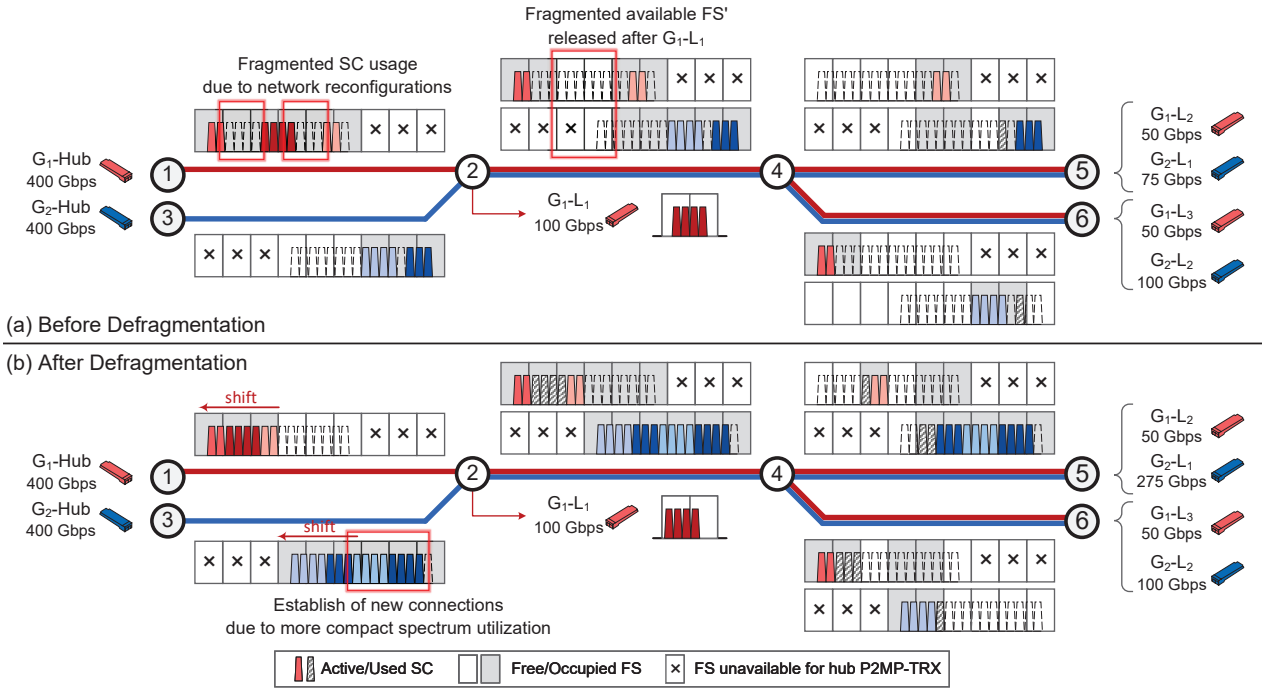

Fig. 1. Example on spectrum saving and reuse enabled by SC-level defragmentation in P2MP-TRX-based WSONs.

LPs to its leaf P2MP-TRXs, each of which only receives the SCs assigned to it. Here, the spectrum allocation granularity of the LPs is a frequency slot (FS), which occupies 12.5 GHz, and each FS can only be allocated to the LPs in one group at most. Note that, although the duplex communications between a hub-leaf P2MP-TRX pair can be routed independently in principle, we assume that they use the same path in both directions for simplicity [19].

An LP request from source s to destination d is modeled as a tuple $r\,(s, d, b, \tau)$, where b and τ denote its bandwidth demand in Gbps and service duration, respectively. For each LP request r, we need to first select an active hub P2MP-TRX, or activate a new hub P2MP-TRX on either s or d to satisfy b. Then, a route between its source and destination is computed, which determines a suitable modulation format m based on its length to ensure the quality-of-transmission (QoT). Finally, SCs from the hub P2MP-TRX are allocated to the corresponding leaf P2MP-TRX. Here, the leaf P2MP-TRXs of a same hub P2MP-TRX should use non-overlapping SCs, which are assumed to be spectrally contiguous according to the operation principle of P2MP-TRXs [23].

Then, after the LPs have been established, SC-level proactive defragmentation can be triggered on-demand or periodically to further improve the efficiency of spectrum and P2MP-TRX utilizations, without incurring excessive reconfigurations. Specifically, each leaf P2MP-TRX can shift its center frequency to receive a different set of SCs from its hub P2MP-TRX, and this can enhance the contiguity of both available FS' and SCs in the WSON. It is worth mentioning that the feasibility of such SC-level reconfiguration has already been verified in recent experimental demonstrations [18].

Fig. 1 gives an illustrative example to explain the further improvement of utilizations of P2MP-TRXs and spectra enabled by the aforementioned SC-level defragmentation. Here, G_n denotes the n-th P2MP group, G_n-*Hub* is the hub P2MP-TRX of the n-th group, and G_n-L_m represents the m-th leaf P2MP-TRX in the n-th group. It can be seen in Fig. 1(a) that when a WSON is built with P2MP-TRXs, spectrum fragmentation due to dynamic LP provisioning will manifest in two both SC and FS levels and can seriously affect the provisioning performance of the WSON. On one hand, spectrum fragmentation leads to isolated small-sized free FS' between the spectrum usages of P2MP-TRX groups. On the other hand, due to the dynamic allocation of SCs, hub P2MP-TRXs may have difficulty to reuse certain SCs and thus need to use more FS' than necessary. In Fig. 1(b), we can see that when SC-level spectrum defragmentation is performed, the impact of spectrum fragmentation can be significantly alleviated and thus more FS' can be reused to provision LP requests.

III. Algorithms Design

In this section, we introduce our proposed TRSA algorithm and the SC-level defragmentation algorithm, which can be triggered proactively to enhance network performance.

A. Transceiver, Routing and Spectrum Assignment

Different from the conventional cases in which LPs are established between P2P-TRX pairs at the same rate, the problem of dynamic provisioning in a P2MP-TRX-based WSON is significantly more complex due to the introduction of additional constraints and sub-problems. The root cause for such difference is that the capacity of each hub P2MP-TRX is

Algorithm 1: P2MP-TRX-based TRSA

```
1  collect network status of WSON G(V, E);
2  while the WSON is operational do
3      restore resources used by expired LP requests;
4      execute SC-level defragmentation in Algorithm 2 on
       demand based on the current network status;
5      get parameters of r_t(s, d, b, τ) and set X_t = ∅;
6      for each active hub P2MP-TRX h ∈ H_s ∪ H_d do
7          for each node v ∈ V_h do
8              for each spur path p' ∈ P_(v,d) do
9                  get available SCs that are from hub
                   P2MP-TRX h and along path p = p' ∪ p_v^h;
10                 if any available SCB can satisfy b then
11                     select the SCB s_h that induces the
                       least additional spectrum usage, and
                       insert tuple {h, p, s_h} in X_t;
12                 end
13             end
14         end
15     end
16     if X_t = ∅ then
17         for each FSB i ∈ [1, Λ − N̂_h + 1)] do
18             get available SCs on links to activate a hub
               P2MP-TRX with the i-th FSB;
19             select a proper hub node v_h ∈ {s, d} as the
               next hub P2MP-TRX h to be activated;
20             for each path p ∈ P_(s,d) do
21                 get availability of the SCs that are from
                   hub P2MP-TRX h and along path p;
22                 if any available SCB can satisfy b then
23                     select the first available SCB s_h and
                       insert tuple {v_h, h, p, s_h} in X_t;
24                 end
25             end
26         end
27     end
28     if X_t ≠ ∅ then
29         execute the best provision scheme in X_t to serve
           r_t, and update network status accordingly;
30     else
31         mark LP request r_t as blocked;
32     end
33 end
```

no longer dedicated to a single LP but shared by the LPs to its leaf P2MP-TRXs. Hence, when a high-speed hub P2MP-TRX is activated to serve a LP request, part of its SCs may remain inactive and can be allocated to subsequent LP requests.

To tackle the dynamic service provisioning in a P2MP-TRX-based WSON, we propose an efficient heuristic as shown in *Algorithm* 1. The algorithm is initialized by collecting network status in *Line* 1, and then the while-loop of *Lines* 2-33 provisions incoming LP requests on-the-fly and performs defragmentation if necessary to optimize the utilizations of spectrum and P2MP-TRXs. In each loop, we first remove the expired LPs and releases their occupied resources, and then decide whether to trigger defragmentation operations (*Lines* 3-4). Here, defragmentation operations can be triggered either periodically, or when a specific parameter (*e.g.*, fragmentation ratio) reaches a preset threshold [24]. The proposed defragmentation method will be elaborated in Section III-B.

Then, *Lines* 5-32 try to serve a pending LP request with the available resources. Specifically, we first try to serve the request with the remaining capacity of active hub P2MP-TRXs (*Lines* 6-15). Here, we leverage the SC tree growth method proposed in [25] to route the LP request so as to prioritize the provisioning schemes that are more spectrally efficient. To do this, we first check each active hub P2MP-TRXs $h \in H_s \cup H_d$, where H_v represents the set of active hub P2MP-TRX on node v. For each hub P2MP-TRX h, we iterate through each node on the current light-tree (*i.e.*, $v \in V_h$) to all of its leaf nodes, and obtain the spur paths $p' \in P_{(v,d)}$ between v and the corresponding leaf node. In *Line* 9, we get $p = p' \cup p_v^h$ as the routing path of the LP request, where p_v^h represents the path between v and the hub node h, and the available SCs on the path are then calculated. If there exists any available SC block (SCB) that can satisfy the bandwidth demand of the request, the SCB s_h that uses the least additional spectrum is chosen, and the corresponding tuple $\{h, p, s_h\}$ is recorded as a candidate provision scheme (*Lines* 10-12).

If none of the active hub P2MP-TRXs can serve the request, we will then seek to activate a new one for the request in *Lines* 16-27. To do this, we first use a for-loop to iterate through all the feasible FS blocks (FSB) in the spectrum domain, obtain the availability of the SCs on each link for each of these FSBs, and thereby determine where to activate the new hub P2MP-TRX (*Lines* 18-19). Here, the size of each FSB is denoted as $\hat{N}_h$, which is the maximum number of FS' that a hub P2MP-TRX can occupy. In *Lines* 20-25, we try to serve the request with pre-computed routing paths, and each possible provision scheme that uses the first available SCB s_h is recorded as a tuple $\{v_h, h, p, s_h\}$. Finally, we select the best provisioning scheme for the request, or it is blocked if a feasible provisioning scheme cannot be found (*Lines* 28-32).

B. SC-level Proactive Spectrum Defragmentation

As discussed above, compared with the cases in P2P-TRX-based WSONs, the negative impact of spectrum fragmentation can be further intensified in P2MP-TRX-based WSONs. Although a fragmentation-aware provisioning scheme can alleviate this issue [20], its effect might still be limited when the LP requests are highly dynamic, and thus the defragmentation approach that leverages LP reconfigurations will be essential to further enhance the utilization of spectrum and P2MP-TRXs.

We propose an SC-level proactive spectrum defragmentation method as shown in *Algorithm* 2, which can be triggered periodically to suppress fragmentation during dynamic provisioning by reconfiguring only leaf P2MP-TRXs. The algorithm takes the network topology $G(V, E)$ and the set of hub-leaf LPs L as input, and outputs the updated SC allocation for L.

Algorithm 2: SC-level Spectrum Defragmentation

Input: Physical topology $G(V, E)$, set of hub-leaf LPs L.
Output: Updated configurations for hub-leaf LPs L.

1 sort all hub-leaf LPs L in ascending order of first the start FS indices of their occupied spectra and then the start indices of their allocated SCs;
2 **for** *each active hub-leaf LP* $l \in L$ **do**
3 obtain all the available FS' $F_{h,l}$ that LP l can use to connect to hub P2MP-TRX h_l on its path p_l;
4 get all the available SCs $S_{h,l}$ for h_l based on $F_{h,l}$;
5 acquire the avaible SCs for l as $S_l = S_{h,l} \wedge U_{h,l}$;
6 shift l to its lowest spectrum allocation according to S_l, and update the spectrum usage along p_l;
7 **end**

In *Line* 1, we sort all the active hub-leaf LPs L in ascending order of first the start FS indices of their occupied spectra and then the start indices of their allocated SCs. Then, the for-loop of *Lines* 2-7 checks each hub-leaf LP in L and attempts to reconfigure it for defragmentation. For each active hub-leaf LP $l \in L$, all the available FS' that it can use to connect to the hub P2MP-TRX h_l along the current routing path p_l is first obtained in the form of a bit vector $F_{h,j}$ (*i.e.*, bit 1 means that an FS is available and bit 0 otherwise) in *Line* 3. Here, the FS' that LP l is currently using are also considered as available. Based on $F_{h,j}$, all the SCs that can be allocated to h_l are then got as a bit vector $S_{h,l}$ (*i.e.*, bit 1 means that an SC is available and bit 0 otherwise), and the SCs that can be used by the hub-leaf LP l are then obtained as $S_l = S_{h,l} \wedge U_{h,l}$, where $\wedge$ denotes the bitwise logical *AND* operation, and $U_{h,l}$ denotes the availability of SCs according to the SC usages of other leaf P2MP-TRXs of h_l (*Lines* 4-5). Finally, the hub-leaf LP l is shifted to its lowest possible spectrum allocation in S_l, and the spectrum usage along p_l is updated accordingly (*Line* 6). The SC-level spectrum defragmentation is over after all the active hub-leaf LPs have been processed.

IV. Performance Evaluations

The simulations use the 14-node Germany topology in [26], assuming that the WSON is based on the flexible-grid with each FS at 12.5 GHz, and each fiber link can accommodates 358 FS' in the C-band [27]. The capacity of each hub P2MP-TRX is assumed to be fixed at 400 Gbps, while that of a leaf P2MP-TRX can be adaptively set according to the bandwidth demand of the request that it serves. Therefore, for each hub P2MP-TRX, its maximum spectrum usage is 6 FS', and it provides 16 SCs, each of which occupies 4 GHz, to its leaf P2MP-TRXs [28]. To emulate dynamic service provisioning in a realistic network environment, we generate non-stationary traffic demands that vary in time and include random short-term fluctuations according to the traffic models in [20, 29]. Specifically, in each time slot, we assume that the arrival of requests follows the Poisson distribution, their lifetimes follows a negative exponential distribution, and the bandwidth demands of the requests are uniformly distributed within $[10, 200]$ Gbps. One FS is reserved as the guard-band on each side of an LP. Dual-polarization 16 quadrature amplitude modulation (DP-16QAM) is adopted if the length of the LP between a hub-leaf pair is within 500 km, and dual-polarization quadrature phase shift keying (DP-QPSK), otherwise [13]. The capacity of an SC is therefore 25 Gbps and 12.5 Gbps with DP-16QAM and DP-QPSK, respectively [13]. The simulations run on Ubuntu servers with 2.1 GHz Intel Xeon Silver 4210R CPU and 32 GB memory, and each data point is obtained by averaging the results from 10 independent runs to ensure sufficient statistical accuracy.

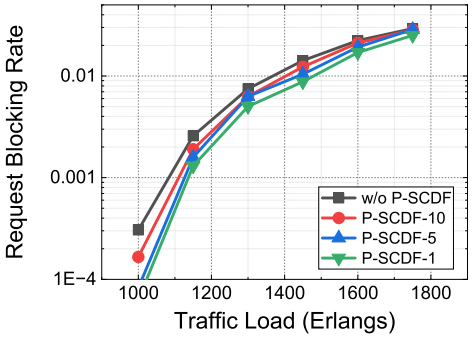

Fig. 2. Results on request blocking rate.

Fig. 2 shows the results on request blocking rate when the proposed SC-level spectrum defragmentation (denoted as P-SCDF) is triggered at different intervals. Here, P-SCDF-N denotes that the SC-level defragmentation is triggered after every N incoming requests, and the scenario without SC-level defragmentation (w/o P-SCDF) is also simulated as a benchmark. We can see that the proposed SC-level defragmentation indeed improves the performance of dynamic provisioning in the WSON, and adopting a shorter network reconfiguration interval can further reduce the blocking probability of requests.

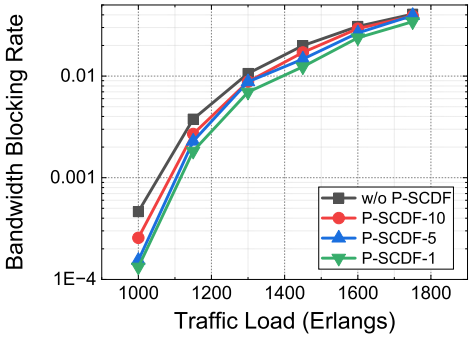

Fig. 3. Results on bandwidth blocking rate.

The results on bandwidth blocking ratio in Fig. 3 further confirm the analysis above. Moreover, we observe that the performance gaps achieved over the case without SC-level defragmentation become larger than those in Fig. 2, suggesting that our proposed SC-level defragmentation can also improve

the fairness in dynamic provisioning. This is because reconfiguring P2MP-TRXs at SC-level can enhance the compactness of LPs in terms of both FS and SC usages, which enables relatively large bandwidth demands to be efficiently served.

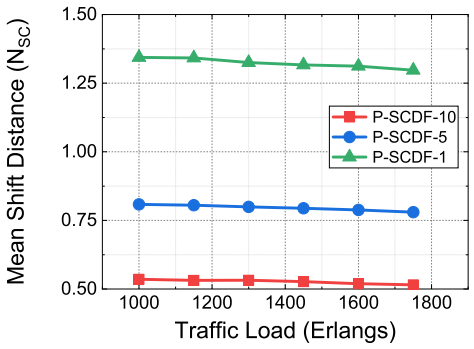

Fig. 4. Mean shift distance.

Finally, we compare the operational complexity at different reconfiguration intervals to explore the trade-off between provision performance and reconfiguration complexity. Fig. 4 shows the mean shift distance of defragmentation operations. Here, the shift distance of a defragmentation operation is defined as the maximum spectrum change in number of SCs among all the reconfigured LPs, denoted as N_{SC}. We notice that although more efficient spectrum utilization can be achieved by using a smaller defragmentation interval, the cost is a significant increase in operation complexity as larger shift distances will be adopted in the defragmentation operations. Hence, a self-adaptive scheme for adjusting the reconfiguration interval might be required to balance the tradeoff between provision performance and operational complexity better [29].

V. Conclusion

This paper tackled the problem of provisioning dynamic traffic demands in a WSON built with P2MP-TRXs. We first proposed an efficient heuristic to handle the TRSA of hub-leaf LPs, and then designed an SC-level proactive spectrum defragmentation algorithm to further enhance the utilizations of spectra and P2MP-TRXs through reconfiguring activated leaf P2MP-TRXs periodically. The effectiveness of our proposals were verified with extensive simulations.

References

[1] P. Lu *et al.*, "Highly-efficient data migration and backup for Big Data applications in elastic optical inter-datacenter networks," *IEEE Netw.*, vol. 29, pp. 36–42, Sept./Oct. 2015.

[2] Z. Pan *et al.*, "Advanced optical-label routing system supporting multicast, optical TTL, and multimedia applications," *J. Lightw. Technol.*, vol. 23, pp. 3270–3281, Oct. 2005.

[3] L. Gong and Z. Zhu, "Virtual optical network embedding (VONE) over elastic optical networks," *J. Lightw. Technol.*, vol. 32, pp. 450–460, Feb. 2014.

[4] S. Li, D. Hu, W. Fang, and Z. Zhu, "Source routing with protocol-oblivious forwarding (POF) to enable efficient e-health data transfers," in *Proc. of ICC 2016*, pp. 1–6, Jun. 2016.

[5] Z. Zhu, W. Lu, L. Zhang, and N. Ansari, "Dynamic service provisioning in elastic optical networks with hybrid single-/multi-path routing," *J. Lightw. Technol.*, vol. 31, pp. 15–22, Jan. 2013.

[6] L. Gong *et al.*, "Efficient resource allocation for all-optical multicasting over spectrum-sliced elastic optical networks," *J. Opt. Commun. Netw.*, vol. 5, pp. 836–847, Aug. 2013.

[7] Y. Yin *et al.*, "Spectral and spatial 2D fragmentation-aware routing and spectrum assignment algorithms in elastic optical networks," *J. Opt. Commun. Netw.*, vol. 5, pp. A100–A106, Oct. 2013.

[8] F. Ji *et al.*, "Dynamic p-cycle protection in spectrum-sliced elastic optical networks," *J. Lightw. Technol.*, vol. 32, pp. 1190–1199, Mar. 2014.

[9] L. Zhang and Z. Zhu, "Spectrum-efficient anycast in elastic optical inter-datacenter networks," *Opt. Switch. Netw.*, vol. 14, pp. 250–259, Aug. 2014.

[10] M. Ju, F. Zhou, S. Xiao, and Z. Zhu, "Power-efficient protection with directed p-cycles for asymmetric traffic in elastic optical networks," *J. Lightw. Technol.*, vol. 34, pp. 4053–4065, Sept. 2016.

[11] J. Back *et al.*, "CAPEX savings enabled by point-to-multipoint coherent pluggable optics using digital subcarrier multiplexing in metro aggregation networks," in *Proc. of ECOC 2020*, pp. 1–4, Dec. 2020.

[12] K. Wu, P. Lu, and Z. Zhu, "Distributed online scheduling and routing of multicast-oriented tasks for profit-driven cloud computing," *IEEE Commun. Lett.*, vol. 20, pp. 684–687, Apr. 2016.

[13] M. Hosseini *et al.*, "Optimization of survivable filterless optical networks exploiting digital subcarrier multiplexing," *J. Opt. Commun. Netw.*, vol. 14, pp. 586–594, Jul. 2022.

[14] L. Gong, Y. Wen, Z. Zhu, and T. Lee, "Toward profit-seeking virtual network embedding algorithm via global resource capacity," in *Proc. of INFOCOM 2014*, pp. 1–9, Apr. 2014.

[15] J. Liu *et al.*, "On dynamic service function chain deployment and readjustment," *IEEE Trans. Netw. Serv. Manag.*, vol. 14, pp. 543–553, Sept. 2017.

[16] L. Gong, H. Jiang, Y. Wang, and Z. Zhu, "Novel location-constrained virtual network embedding (LC-VNE) algorithms towards integrated node and link mapping," *IEEE/ACM Trans. Netw.*, vol. 24, pp. 3648–3661, Dec. 2016.

[17] Z. Zhong *et al.*, "Provisioning short-term traffic fluctuations in elastic optical networks," *IEEE/ACM Trans. Netw.*, vol. 27, pp. 1460–1473, Aug. 2019.

[18] D. Welch *et al.*, "Digital subcarrier multiplexing: Enabling software-configurable optical networks," *J. Lightw. Technol.*, vol. 41, pp. 1175–1191, Feb. 2023.

[19] Y. Zhang *et al.*, "Planning of survivable wavelength-switched optical networks based on p2mp transceivers," *IEEE Trans. Netw. Serv. Manag., in Press*, pp. 1–12, 2023.

[20] R. Li, Q. Lv, and Z. Zhu, "Architecting wavelength-switched optical networks with coherent P2MP transceivers," in *Proc. of ICOCN 2023*, pp. 1–3, Aug. 2023.

[21] L. Velasco *et al.*, "Autonomous and energy efficient lightpath operation based on digital subcarrier multiplexing," *IEEE J. Sel. Areas Commun.*, vol. 39, no. Sept., pp. 2864–2877, 2021.

[22] W. Shi, Z. Zhu, M. Zhang, and N. Ansari, "On the effect of bandwidth fragmentation on blocking probability in elastic optical networks," *IEEE Trans. Commun.*, vol. 61, pp. 2970–2978, Jul. 2013.

[23] M. Iqbal *et al.*, "Supporting heterogenous traffic on top of point-to-multipoint light-trees," *Sensors*, vol. 23, no. 5, p. 2500, 2023.

[24] R. Li, R. Gu, W. Jin, and Y. Ji, "Learning-based cognitive hitless spectrum defragmentation for dynamic provisioning in elastic optical networks," *IEEE Commun. Lett.*, vol. 25, pp. 1600–1604, May 2021.

[25] P. Pavon-Marino, N. Skorin-Kapov, and A. Napoli, "Tree-determination, routing, and spectrum assignment using point-to-multipoint coherent optics," *J. Opt. Commun. Netw.*, vol. 15, pp. C29–C40, Jul. 2023.

[26] J. Pedro, N. Costa, and S. Sanders, "Cost-effective strategies to scale the capacity of regional optical transport networks," *J. Opt. Commun. Netw.*, vol. 14, pp. A154–A165, Feb. 2022.

[27] C. Chen *et al.*, "Demonstrations of efficient online spectrum defragmentation in software-defined elastic optical networks," *J. Lightw. Technol.*, vol. 32, pp. 4701–4711, Dec. 2014.

[28] P. Pavon-Marino *et al.*, "On the benefits of point-to-multipoint coherent optics for multilayer capacity planning in ring networks with varying traffic profiles," *J. Opt. Commun. Netw.*, vol. 14, pp. B30–B44, May 2022.

[29] M. Zhang, C. You, H. Jiang, and Z. Zhu, "Dynamic and adaptive bandwidth defragmentation in spectrum-sliced elastic optical networks with time-varying traffic," *J. Lightw. Technol.*, vol. 32, pp. 1014–1023, Mar. 2014.